Journal of Solid State Chemistry 184 (2011) 3185–3189

Contents lists available at SciVerse ScienceDirect

Journal of Solid State Chemistry

journal homepage: www.elsevier.com/locate/jssc

Structure and properties of rhombohedral $CePd_3Ga_8$: A variant of the cubic parent compound with $BaHg_{11}$ structure type

Robin T. Macaluso [a,b,*], Melanie Francisco [c], David P. Young [d], Shane Stadler [d], John F. Mitchell [b], Urs Geiser [b], Han-yul Hong [a], Mercouri G. Kanatzidis [b,c]

[a] Department of Chemistry and Biochemistry, University of Northern Colorado, Greeley, CO 80639, USA
[b] Materials Science Division, Argonne National Laboratory, 9700S. Cass Ave., Argonne, IL 60439, USA
[c] Department of Chemistry, Northwestern University, Evanston, IL60208, USA
[d] Department of Physics and Astronomy, Louisiana State University, Baton Rouge, LA 70803, USA

ARTICLE INFO

Article history:
Received 26 July 2011
Received in revised form
30 September 2011
Accepted 2 October 2011
Available online 8 October 2011

Keywords:
$BaHg_{11}$ type
Flux growth
Single-crystal X-ray diffraction
Intermetallic
$CePd_3Ga_8$

ABSTRACT

Single crystals of a new intermetallic gallide, *R*-$CePd_3Ga_8$, have been synthesized from excess molten gallium. Single-crystal X-ray diffraction reveals that *R*-$CePd_3Ga_8$ crystallizes in the *R-3m* space group with $a=b=c=8.4903(10)$ Å and $\alpha=\beta=\gamma=89.993(17)$. *R*-$CePd_3Ga_8$ is a variant of the cubic $BaHg_{11}$ structure type with three structural units: a Ce-centered polyhedron, a distorted cube of Pd_2Ga_6 and a Pd-centered cuboctahedron. The distortions of these units are compared to undistorted analogous units in intermetallic compounds with $BaHg_{11}$ structure type. Field and temperature-dependent magnetization measurements on *R*-$CePd_3Ga_8$ reveal a paramagnetic material with strong antiferromagnetic correlations and a magnetization consistent with Ce^{3+}. Electrical resistance measurements indicate Kondo behavior between localized Ce^{3+} magnetic moments.

1. Introduction

The class of polar intermetallics lies between the well-known Hume-Rothery and Zintl phases [1–3] and for this reason presents a change in understanding their structures and bonding. Hume-Rothery phases are composed of Group 11 metals combined with Group 12–15 elements, and their crystal structures can be rationalized by valence electron count [4]. Zintl phases, on the other hand, have significantly large electronegativity differences and their structural features can be understood with the octet rule. As in Zintl phases, polar intermetallics also possess large electronegativity differences between constituent metals. However, their structural features cannot be easily rationalized.

In Group 13 intermetallics, aluminides are generally considered to be at the so-called Zintl phase boundary, whereas gallides are often not considered to be Zintl phases [3]. Since Al and Ga are isoelectronic, it would be reasonable to expect that intermetallic aluminides and gallides would form similar structures; however, there are actually very few examples of isostructural Al and Ga compounds. This implies that there is a significant contrast between aluminides versus gallides, and that the continued investigation of intermetallic gallium compounds is warranted. Synthesis and characterization of novel gallides may also facilitate a better understanding of the wide spectrum of bonding in intermetallics with Hume-Rothery phases characterizing one extreme and Zintl phases characterizing the other.

Polar intermetallics are often characterized by complex structures. A rich and diverse range of Ga-clusters can be formed in alkali metal-gallides, including dumbbells, icosahedra, and Samson polyhedra [1]. However, gallide clusters are generally considered complex and their chemistry still remains a challenge to the scientific community. Gallium intermetallics exhibit a wide range of interesting structure, physical properties and potential applications, ranging from heavy-fermion magnetic to semihydrogenation catalysts [5–9].

In our investigations, we have identified rhombohedral *R*-$CePd_3Ga_8$ and cubic *C*-$CePd_3Ga_8$ variants of the $BaHg_{11}$ structure type. In this paper, we report for the first time the synthesis and structure of single crystals of the *R*-$CePd_3Ga_8$. Several aluminides bearing the $BaHg_{11}$or closely related structure include $CeAg_3Al_8$ [10], $EuAg_xAl_{11-x}$ [11], $RAu_{6+x}Al_{26}T$ (R=Ca, Sr, Eu, Yb; T=early transition metal) [12], and $M_3Au_{6+x}Al_{26}Ti$ (M=Ca, Sr, Yb) [13]. $CePd_3Ga_8$ will provide opportunities to investigate the similarities and differences in aluminide versus gallide chemistry.

---

* Corresponding author at: Department of Chemistry and Biochemistry, University of Northern Colorado, Ross Hall, Campus Box 98, Greeley, CO 80639, USA.
E-mail address: robin.macaluso@unco.edu (R.T. Macaluso).

0022-4596/$ - see front matter © 2011 Elsevier Inc. All rights reserved.
doi:10.1016/j.jssc.2011.10.001

2. Materials and methods

2.1. Synthesis

Cerium (Alfa Aesar, 99.9%), palladium (Alfa Aesar, 99.95%), and gallium (Alfa Aesar, 99.999%) were used to synthesize single crystals of $CePd_3Ga_8$. Cerium powder was obtained from filing a Ce ingot in a N_2-filled glove box, where the powder from the surface was discarded, and only Ce powder from the interior of the ingot was used in the synthesis reactions. Palladium and gallium were used as received.

Ce filings, Pd, and Ga were added to an alumina crucible in a 1:2:20 molar ratio. The crucible and its contents were sealed in a fused silica ampoule, and then heated to 1150 °C at 65°/h in a box furnace. The ampoule dwelled at 1150 °C for 2 h before being cooled to 350 °C at a rate of 60 °C/h. The ampoule was removed from the furnace at 350 °C, and immediately inverted and placed into a centrifuge. Cooling and removing the ampoule at 300 °C yielded similar results.

Alternatively, single crystals were obtained by heating to 1000 °C, dwelling for 5 h, slow-cooling to 860 °C at 5.83 °C/h, dwelling for 60 h, and fast-cooling to 300 °C at 75 °C/h. At 300 °C, the tube was quickly inverted and centrifuged at 2800 rpm to remove excess flux. The major phase was $CePd_3Ga_8$, which was approximately 80–90% of the final product, with 10–20% of the final product as minority phases, $CePdGa_6$ and Ce_2PdGa_{12}. Yields were determined by relative intensities in powder X-ray diffraction patterns.

The excess liquid Ga was removed by centrifugation of the inverted ampoule for 3–5 min. An image of a typical crystal obtained by scanning electron microscopy is shown in Fig. 1. Single crystals in the alumina crucible were mechanically extracted for structural analysis and property measurements. Crystal dimensions ranged between 0.50 to 0.75 mm, with flat surfaces corresponding to the 1-1-1 face. Residual Ga flux remaining on the crystal surface was removed by placing the crystals in a 3M solution of I_2 in DMF. Crystals appeared to be stable in air for at least several months.

2.2. Diffraction

The crystal structure of $CePd_3Ga_8$ was determined using single-crystal X-ray diffraction. A $0.01 \times 0.01 \times 0.01\ mm^3$ fragment was placed on a glass fiber with epoxy and centered in an X-ray beam with a Bruker SMART CCD diffractometer equipped with Mo K_α radiation ($\lambda = 0.71073$ Å) and area detector. Experimental parameters are included in Table 1. Data processing of the full data sets were performed using the program SAINT. Absorption corrections were made using SADABS [14], and crystal symmetry analysis was performed with XPREP [15]. The structure solution was obtained by direct methods and then refined by full-matrix-least-squares with the SHELXTL suite of programs [15]. Anisotropic atomic displacement parameters were refined for each site.

Table 1
Structural refinement data for R-$CePd_3Ga_8$.

Formula	$CePd_3Ga_8$
Formula mass (amu)	1017.8
Space group	$R\text{-}3m$
$a=b=c$(Å)	8.4903(10)
$\alpha=\beta=\gamma$	89.993(17)
V (Å^3)	612.02(12)
Z	3
T (K)	293(2)
ρ (calculated)	8.282
Crystal dimensions (mm)	$0.01 \times 0.01 \times 0.01$
Radiation	Graphite monochromated Mo$K\alpha$
μ (mm^{-1})	37.735
$2\theta_{maximum}$ (°)	56.52
Collected reflections	1920
Unique reflections, with $F_o^2 > 2\sigma(F_o^2)$	561
h	$-11 \le h \le 11$
k	$-8 \le k \le 5$
l	$-11 \le l \le 5$
No. of variables	39
$R(F)$ for F_o^2	0.0330
$R_w(F_o^2)$	0.0742
Extinction coefficient	0.010475
$(\Delta_\rho)_{max}$, $(\Delta_\rho)_{min}$ (e Å^{-3})	1.833, −2.975

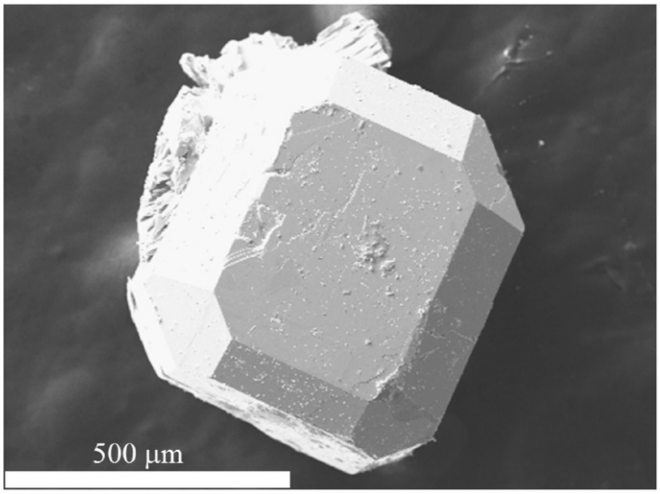

Fig. 1. An image of a typical flux-grown crystal of R-$CePd_3Ga_8$ obtained by SEM methods. The scale bar shown at the bottom of the image represents 500 μm.

2.3. Elemental analysis

Elemental analysis was performed using a JEOL JSM-6610LV scanning electron microscope with energy-dispersive X-ray spectroscopy (EDX) capabilities. Crystals were mounted on an aluminum stub covered with carbon tape. Semi-quantitative analyses were performed on crystals using 20 kV accelerating voltage and an accumulation time of 180 s. Analyses of multiple spots on several crystals reveal an average composition of R-$Ce_{1.10(2)}Pd_{3.5(2)}Ga_{7.4(2)}$.

2.4. Electrical resistivity

The temperature dependence of the electrical resistance of a single crystal of $CePd_3Ga_8$ was measured using a standard 4-probe AC technique in a Quantum Design Physical Properties Measurement System (PPMS). Two-mil diameter Pt wires were attached to the sample with a 2-component conductive silver epoxy (Epotek H20E). Typical excitation currents were ~0.5 mA at a frequency of 27 Hz.

2.5. Magnetic susceptibility

The temperature-dependent magnetic susceptibility and field-dependent magnetization data were measured with a Quantum Design MPMS XL SQUID magnetometer. A single crystal was mounted in a plastic drinking straw and field-cooled (FC) in an applied field of 1000 Oe. The magnetization was then measured at 3 K in fields from 0 to 5 T.